FULL PAPER

Dalton
www.rsc.org/dalton

Reactivity of the tetraphenyldithioimidodiphosphine–diiodine ($HL·I_2$) adduct towards indium powder

G. Luca Abbati,[b] M. Carla Aragoni,[a] Massimiliano Arca,[a] F. A. Devillanova,[a]
Antonio C. Fabretti,[b] Alessandra Garau,[a] Francesco Isaia,*[a] Vito Lippolis[a] and G. Verani[a]
[a] *Dipartimento di Chimica Inorganica ed Analitica, Università di Cagliari, S.S. 554 bivio per Sestu, I-09042 Cagliari, Italy*
[b] *INSTM and Dipartimento di Chimica, Università di Modena e Reggio Emilia, via G. Campi 183, I-41100 Modena, Italy*

Received 28th November 2002, Accepted 26th February 2003
First published as an Advance Article on the web 11th March 2003

The reaction of indium powder with the mixture $(SPPh_2)_2NH$ and I_2 ($HL·I_2$) in Et_2O at room temperature gave the indium(III) complex $InLI_2$ (**1**). The reaction occurs in two steps, the first of which leads to the formation of InI_3 and free **HL**, then the subsequent reaction between these species yields compound **1**, H^+, and the anion InI_4^-. The crystal lattice of **1** is made up of neutral acentric molecules where the metal ion is bonded through two sulfur atoms to one anionic $(SPPh_2)_2N^-$ (**L**) ligand and two iodide ions. The central In^{III} ion shows a slightly distorted tetrahedral coordination geometry. Density functional theory (DFT) calculations, carried out at the B3LYP level, have been used to interpret the electrochemical behaviour of **1**.

Introduction

The chemistry of metal powder activation by CT-adducts of halogen and interhalogen has been widely developed by McAuliffe and co-workers during the past ten years.[1] Owing to the main use of $R_3E·X_2$ adducts (R = alkyl, aryl; E = P, As, Sb; X_2 = I_2, Br_2, IBr), novel metal tertiary phosphine, arsine, and stibine complexes were prepared. The versatility of this synthetic method allows one to prepare coordination compounds having unusual geometries, stoichiometries, and oxidation number at the metal centres. Furthermore, it points the way towards a safe, clean technology for the recovery of precious metals.[2] In this way, the metal activation reaction using I_2-adducts of polyfunctional thione donors has been carried out to produce complexes such as $[Pt(Me_2Pipdt)_2](I_3)_2$ (Pipdt = *N,N′*-dimethylpiperazinium-2,3-dithione),[2] $[AuDI_2]I_3$ (D = *N,N′*-dimethylperhydrodiazepine-2,3-dithione),[3] and some $SnI_2(D')_2(I_3)_2·2/3I_2$ (D′ = 1,1′-bis(3-methyl-4-imidazolidine-2-thione).[4]

In this context, the diiodine adducts of tetraphenyldithioimidodiphosphinic acid $(SPPh_2)_2NH$ (**HL**) represents an interesting system for activating metal powder since it contains Group 15 and 16 donor elements. The coordination chemistry of **HL**, and more in general of some imidodiphosphinic acids $(XPR_2)(YPR'_2)NH$ (X, Y = O, S; R, R′ = Me, Pr^i, Ph), has already been investigated[5] thoroughly and some complexes have found application as catalysts for methanol carbonylation.[6]

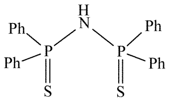

HL

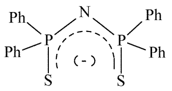

L

The reaction of **HL** with metal ions usually leads to the formation of the $(SPPh_2)_2N^-$ anion (**L**) which has the negative charge delocalised over the SPNPS moiety, and is capable of coordinating a metal centre by both sulfur atoms to form six-membered $MSSP_2N$ metallacycles. Square planar, tetrahedral, or octahedral complexes of formula ML_n (n = 2 or 3) are the most commonly observed coordination geometries.[7] In some cases, more complicated stoichiometries have been obtained with formation of bridges or supramolecular polymeric structures.[8,9]

In previous papers[7a,b,8a] we reported on the oxidation ability of the mixture of **HL** and I_2 towards metal powders in a low polar solvent and mild reaction conditions. Sb^0 is easily oxidised to +3 in a single step to separate an unusual dinuclear complex $[\mathbf{L}Sb(\mu\text{-}S)(\mu\text{-}I)_2Sb\mathbf{L}]$.[8a] Similarly, the same mixture has successfully been used to react palladium and cobalt powders to produce the complexes $Pd\mathbf{L}_2$[7a] and $Co\mathbf{L}_2$.[7b]

Considering these promising results and given the importance of indium complexes in view of their applications in organic synthesis as catalysts in trans-esterification processes,[10] and the increasing interest in the recovery process of indium from scrap and waste products from the electronics industry,[11] we report on the activation of indium powder by the mixture **HL** and I_2.

Results and discussion

Solid-state structure

Stable colourless crystals suitable for an X-ray study were obtained by reaction of **HL**, I_2 and indium powder (see Experimental section, synthesis method a) in anhydrous diethyl ether at room temperature. The crystal lattice is made up of neutral acentric $In\mathbf{L}I_2$ (**1**) molecules where the metal ion is bonded through two sulfur atoms to one anionic ligand $(SPPh_2)_2N^-$ (**L**) and two iodide ions (Fig. 1). The central In^{III} ion shows a slightly distorted tetrahedral coordination geometry with X–In–X angles (X = I, S) in the range 102.28(3)–115.57(3)° (see Table 1) and a dihedral angle between the I(1)In(1)I(2) and S(1)In(1)S(2) planes of 83.73(2)°. The pronounced difference observed in the mean values of the In–S and In–I bond-lengths (2.485 and 2.682 Å, respectively) is probably due to the arrangement of the sterically restrained S ··· S ligand "bite" in the metal ion coordination geometry. The In–I distances are in fact equal, within experimental errors, to the value of 2.64(4) Å reported as the usual In^{III}–I mean distance in four-coordinated pseudo-tetrahedral complexes.[12] To our knowledge, **1** is the first example of an indium–iminobis(phosphinechalcogenide) complex showing a tetrahedral metal coordination geometry. All the previously studied indium complexes with such ligands in fact showed an octahedral[13] or trigonal bipyramidal geometry.[14] In **1** the InSPNPS ring adopts a pseudo-boat conformation where atoms S(1) and P(2) act as "bow" and "stern", with deviations of 0.8798(14) and

DOI: 10.1039/b211542e

Table 1 Selected interatomic distances (Å) and angles (°) for complex **1**

In(1)–S(1)	2.4841(12)	In(1)–S(2)	2.4863(10)
In(1)–I(1)	2.6769(5)	In(1)–I(2)	2.6872(6)
S(1)–P(1)	2.0452(13)	S(2)–P(2)	2.0478(12)
P(1)–N(1)	1.585(3)	P(2)–N(1)	1.578(3)
P(1)–C(7)	1.793(4)	P(1)–C(1)	1.794(4)
P(2)–C(13)	1.788(3)	P(2)–C(19)	1.805(3)
I(1) ··· I(2)	4.4781(8)	S(1) ··· S(2)	4.041(2)
I(1) ··· S(1)	4.3677(13)	I(2) ··· S(2)	4.2627(11)
I(1) ··· S(2)	4.1284(11)	I(2) ··· S(1)	4.0287(13)
I(1)–In(1)–I(2)	113.20(2)	S(1)–In(1)–S(2)	108.77(3)
S(1)–In(1)–I(1)	115.57(3)	S(2)–In(1)–I(2)	110.90(3)
S(2)–In(1)–I(1)	106.12(3)	S(1)–In(1)–I(2)	102.28(3)
P(1)–S(1)–In(1)	98.60(5)	P(2)–S(2)–In(1)	100.00(4)
N(1)–P(1)–S(1)	117.03(12)	N(1)–P(2)–S(2)	116.22(13)
P(2)–N(1)–P(1)	132.7(2)		
N(1)–P(1)–C(1)	109.2(2)	N(1)–P(1)–C(7)	107.6(2)
C(1)–P(1)–S(1)	108.72(13)	C(7)–P(1)–S(1)	107.05(14)
C(7)–P(1)–C(1)	106.8(2)		
N(1)–P(2)–C(13)	106.5(2)	N(1)–P(2)–C(19)	112.5(2)
C(13)–P(2)–S(2)	105.22(12)	C(19)–P(2)–S(2)	109.19(13)
C(13)–P(2)–C(19)	106.5(2)		

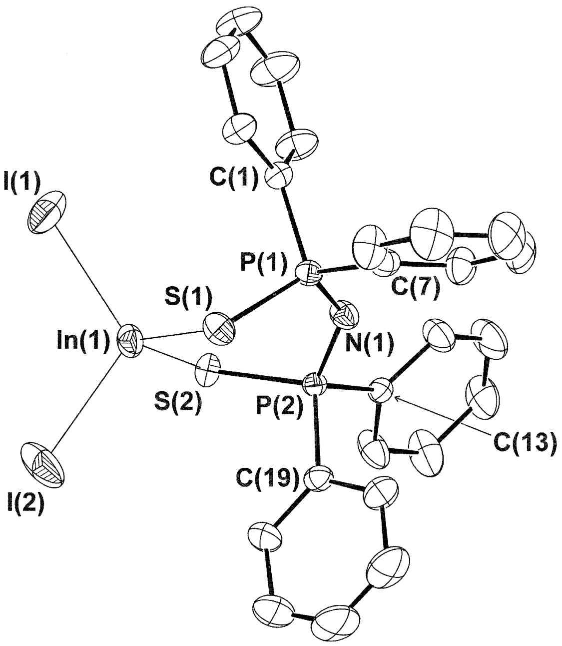

Fig. 1 ORTEP[27e] plot of **1** showing the atom labeling scheme and 30%-probability thermal ellipsoids. Hydrogen atoms have been omitted for clarity.

0.756 (2) Å, respectively, from the mean In(1)P(1)N(1)S(2) plane and dihedral angles between the named plane and In(1)P(1)S(1) [S(2)N(1)P(2)] of 39.13(7)° [49.91(9)°]. Interestingly, the conformation of the InSPNPS ring seems to be controlled by the steric hindrance of the bulky $(SPR_2)_2N$ ligands (R = Ph,[13,14b] Pr^i [14a]) rather than by the coordination number of the indium ion. Despite the different coordination geometries the rings in fact show the same overall boat conformation in **1**, InL_3 (**2**)[13a] and $InCl((SPPr^i{}_2)_2N)_2$ (**3**) (Fig. 2),[14a] although a "flipping" of the InSPNPS ring is observed upon increasing the steric requirements of the ligand molecule arrangement around the metal ion, on passing from **1** to **2**, and **3** (where N and In act as bow/stern of the ring). Though far from being planar [deviations from the mean plane ± 0.5537(13) Å], the geometry of the InSPNPS moiety clearly shows a π-electron delocalisation over the whole ring as a result of metal coordination, in a way already observed in various metal–$(XPR_2)_2N$ complexes (R = Ph, Me, Pr^i; X = S, Se, O).[7a,13,14] In **1** in particular, on comparing with the free ligand **HL**,[15] the P–S distances increase from 1.937(1)–1.950(1) to 2.0452(13)–2.0478(12) Å, while the P–N bond lengths decrease [1.672(2)–1.683(2) *vs.* 1.578(3)–1.585(3) Å] and the P–N–P angle is practically the same [132.7(2) *vs.* 132.68(14)°]. These values substantially confirm that the bond geometry of the metal–$(XPR_2)_2N$ fragment is insensitive to the oxidation number and coordination environment of the involved metal ion.[7a]

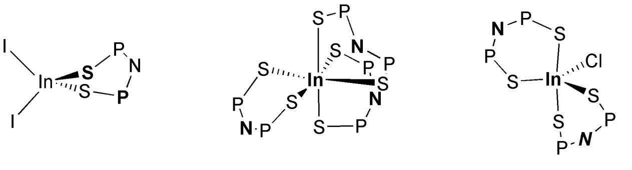

$InLI_2$ (**1**) InL_3 (**2**) $InCl((SP^iPr_2)_2N)_2$ (**3**)

Fig. 2 Simplified chemical structure representations of the InPSNPS ring in **1**, **2**, and **3**. Bold-printed atoms act as 'bow' or 'stern' of the pseudo-boat conformation shown by the rings.

The ^{31}P MAS NMR spectrum of the indium complex **1** shows two resonances at δ 36.8 and 41.3 with an approximate intensity ratio of 1 : 1 originated from the non-equivalent P sites of the ligand within the complex. Peaks have a line width $\Delta\nu_{1/2}$ of ≈300 Hz, thus excluding the possibility of observing any $^2J(^{31}P, ^{31}P)$ [≈25 Hz in this class of ligands]. The inequivalence of the P sites in the ligand moiety is not found in diethyl ether solution, in fact the ^{31}P spectrum of $InLI_2$ (1.3×10^{-2} mol dm^{-3}, 25 °C) is a sharp singlet (δ 38.1, $\Delta\nu_{1/2}$ = 3.5 Hz), and both δ and $\Delta\nu_{1/2}$ are substantially unaffected in the temperature range +40 to −55 °C, the latter being the lowest temperature for which ^{31}P NMR data were available. No ^{115}In NMR resonance was detected with a solution of **1** in diethyl ether. Owing to the high nuclear spin of indium, we were not able to detect any ^{115}In NMR signal in accordance with the fact that only In^{III}-containing species with high symmetry are detectable.[16]

IR spectroscopy agrees with structural and NMR data. The P=S bonds are lengthened and the P–N bonds are shortened compared to the ligand **HL** as a consequence of the electron delocalisation associated with deprotonation/complexation. The ν(P–S) stretching bands in the complex (566 and 523 cm^{-1}) agree with a reduced P–S bond order compared to the free ligand **HL** (689 and 650 cm^{-1}).[17] The ν_{asym}(PNP) (1240 cm^{-1}), which is the most sensitive band to ligand complexation, is indicative of an increased bond order with respect to the free ligand (922 cm^{-1}).[17]

UV-Vis and NMR solution studies

The reaction between **HL**, I_2 and In (1 : 1.5 : 1 molar ratio; **HL** = 2.22×10^{-3} mol dm^{-3}, 25 °C) in diethyl ether differs from those carried out with the metals Co^0, Pd^0, and Sb^0, in that the typical dark-red colour of the reaction mixture, due to the immediate formation of the charge-transfer adduct bearing the S–I–I group, rapidly disappears. In fact, on monitoring the course of the reaction by the blue-shifted band of iodine[18] at 460 nm, it appears clear that the concentration of the adduct $HL\cdot I_2$ lowers during the first hour of reaction and becomes negligible within ninety minutes. At this stage of the reaction, ^{115}In and ^{31}P NMR spectroscopy show signals at $\delta(^{115}In)$ −1020 ($\Delta\nu_{1/2}$ = 775 Hz) and $\delta(^{31}P)$ 57.1. This strongly indicates the formation of indium triiodide[16,19] and free **HL**.[5f] In the course of the reaction, the ^{31}P NMR signal related to **HL** decreases in intensity and the formation of a new signal at δ 38.1 is observed at the same time. After one day the solution does not undergo any further reaction, about 60% of the initially formed **HL** is still present unreacted in the solution (Fig. 3a). The chemical shift at δ 38.1 indicates formation of a deprotonated ligand-containing species, according to the upfield shift of *ca.* 19 ppm of the ^{31}P NMR signal upon complexation of **HL**.[5f] Assignment of this signal to the species $InLI_2$ is confirmed by comparison with the spectrum of the neat compound dissolved in Et_2O showing a signal at δ 38.1.

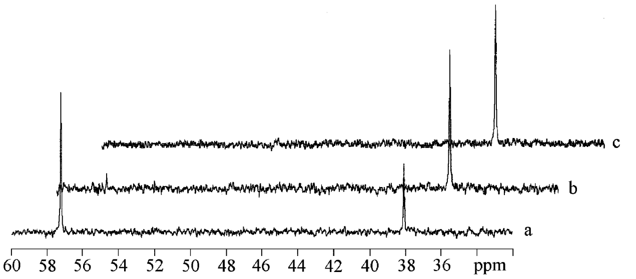

Fig. 3 ^{31}P NMR spectra in Et_2O at 25 °C of the reaction mixtures **HL**, I_2, and In at different molar ratios recorded after 7 days. Molar ratios: 1 : 1.5 : 1; 1 : 3 : 2; 1 : 4.5 : 3, for a, b, and c, respectively; **HL** = 2.22 × 10^{-3} mol dm^{-3}.

Based on these results we also synthesised complex **1** (see Experimental section, synthesis method b) by using indium triiodide and **HL** as reagents. We found that the yield of this reaction is slightly lower than that based on indium powder, moreover, we reckon that the possibility of generating indium triiodide *in situ* easily (see Experimental section, synthesis method a) is a great advantage as this compound is itself very air-sensitive. At present the influence exerted by the mixture of **HL** and I_2 in the process of oxidation of the metal is still not fully understood,[7a] although it is recognisable from a qualitative experimental basis that indium powder reacts with I_2 more quickly in the presence of **HL**.

In order to elucidate its stoichiometry, we also monitored the reaction by ^{31}P NMR starting from **HL**, I_2, and In in a 1 : 3 : 2 molar ratio (**HL** = 2.22 × 10^{-3} mol dm^{-3}, 25 °C) in order to obtain a higher InI_3 to **HL** reaction molar ratio. The ^{31}P NMR spectrum of the mixture recorded after 7 days shows one peak at δ 38.1 and a very small peak at δ 57.1. In this case the formation of $InLI_2$ is almost quantitative (Fig. 3b). By starting from an **HL**, I_2 and In 1 : 4.5 : 3 molar ratio, the only peak observable after 7 days in the ^{31}P NMR spectrum is that at δ 38.1 (Fig. 3c). Interestingly for all reaction molar ratios employed, the ^{115}In NMR spectrum measured at the end of the reaction supports the formation of a new indium-containing species different from InI_3 and **1**. In fact, a resonance at δ −1022 (Et_2O, $\Delta\nu_{1/2}$ = 520 Hz) is observed which indicates formation of the tetraiodoindate anion InI_4^-;[20,21] Raman peaks at 184w and 138vs cm^{-1} confirming the presence of this species.[22]

Therefore, it can be hypothesised that the reaction between the adduct and indium powder occurs in two subsequent steps. One leads to the formation of indium triiodide [eqn. (1)],

$$\mathbf{HL}\cdot I_2 + 2I_2 + 2In \xrightarrow{Et_2O} In_2I_6 + \mathbf{HL} \qquad (1)$$

which is known to exist exclusively as dimer In_2I_6 in non-coordinating solvents;[20,21] while the other consists of the reaction of this species with **HL** to yield the stable complex $InLI_2$ (**1**) [eqn. (2)].

$$In_2I_6 + \mathbf{HL} \xrightarrow{Et_2O} In\mathbf{L}I_2 + H^+ + InI_4^- \qquad (2)$$

Unlike the previously studied reactions of **HL** and I_2 with cobalt and palladium metal powders, where we were able to identify the intermediate species CoI_2·**HL** and PdI_2·**HL** respectively, in this case the formation of the 1 : 1 adduct InI_3·**HL** was not detected, not even by reacting indium triiodide and **HL** at −40 °C. Moreover, the possibility of preparing InI_3·**HL** by addition of HI to a solution of $InLI_2$ (1.3 × 10^{-2} mol dm^{-3}, Et_2O, 25 °C) was also verified. Conversely, this reaction leads to the release of the free ligand **HL**, as shown by the ^{31}P NMR chemical shift change to 57.1 from 38.1 ppm and the formation of the anion InI_4^-. The latter reaction might be very important for an indium-recovery process from industry residues based on eqns. (1) and (2); in fact, it provides the way to free the metal from **1** as InI_4^- species, which are easily separable as salts from the solution of **HL**, which can be re-utilised.

Interestingly, it is possible to start from the caesium salt Cs**L**, instead of **HL** itself, to prepare **1** with a higher yield and a shorter reaction time. This result is not unexpected because of the higher nucleophilicity of **L** compared to **HL** (the calculated NBO charges on the sulfur donor atoms of the $(SPH_2)_2NH$ model ligand **HL**′ are −0.707 and −0.496 e for **L**′ and **HL**′ respectively).[7a,7b] The ^{31}P NMR spectrum of a mixture of Cs**L**, I_2, and indium metal powder (1 : 1.5 : 1 molar ratio) in anhydrous diethyl ether recorded after one day is reported in Fig. 4. Although the reaction carried out with Cs**L** has a higher yield in complex **1** compared to the use of **HL**, one of its main drawbacks is the formation of by-products, which were not identified (starred peaks in Fig. 4). Moreover, a partial hydrolysis of the monohydrate salt Cs**L**·H_2O regenerates the **HL** species.

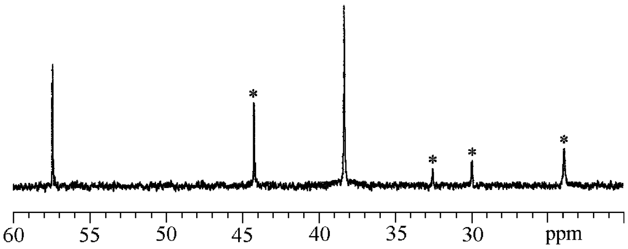

Fig. 4 ^{31}P NMR spectrum in Et_2O at 25 °C of the reaction mixture of Cs**L**, I_2, and In (1 : 1.5 : 1 molar ratio) recorded after 1 day. The peaks labeled with a star are due to unidentified species.

We also tried to synthesise complexes with a higher ligand content by reacting an excess of Cs**L** with a solution of $InLI_2$ in Et_2O, but complex **1** remained the only isolated species.

Redox properties and theoretical calculations

The redox properties of **1** have been measured by cyclic voltammetry in CH_3CN (0.1 mol dm^{-3} in Bu_4NBF_4) in the range +1.6 to −1.6 V where the ligand **HL** is electrochemically inactive. Two irreversible coulometrically-tested monoelectronic reductions at E_{pc1} = −0.65 V and E_{pc2} = −1.2 V *vs.* Ag/AgCl were observed and can be assigned to the couples In^{III}/In^{II} and In^{II}/In^{I}, respectively. In addition, one irreversible bielectronic oxidation was observed at E_{pa} = +0.51 V *vs.* Ag/AgCl, due to the couple $2I^-/I_2$. Interestingly, indium triiodide in CH_3CN exhibits a cyclic voltammogram similar to that of **1**, with two irreversible reduction processes at E_{pc1} = −0.35 V and E_{pc2} = −0.85 V and one irreversible oxidation at E_{pa} = +0.98 V *vs.* Ag/AgCl.

The non-bonding Kohn–Sham[23] HOMO (Fig. 5) and the HOMO − 1, involved in the reduction processes, have been calculated on the model complex $In\mathbf{L}'I_2$ (**4**) [**L**′ = $(SPH_2)_2N^-$] in which the bulky phenyl groups have been replaced by hydrogen atoms, and are simply formed by the combination of the two corresponding iodine p_x and p_y atomic orbitals. The LUMO (Fig. 5), involved in the oxidation process, is a σ* antibonding molecular orbital with a very large contribution of the valence shell s indium atomic orbital interacting with the p_z atomic orbitals of the four donor atoms. It should be pointed out that the HOMO and LUMO calculated at the same level of theory for InI_3 in its dimeric form show analogous compositions. Although the changes in the thermodynamic parameters involved in the redox processes are neglected, the lower Kohn–Sham LUMO eigenvalue calculated for In_2I_6 compared to that calculated for **4** (ε_{LUMO} = −0.147 and −0.087 Hartree, respectively) (Fig. 5) explains the easier reduction process observed for In_2I_6. The nature of the LUMO implies that the reductions in both compounds are mainly centred on the In atom (In^{III}/In^{II}

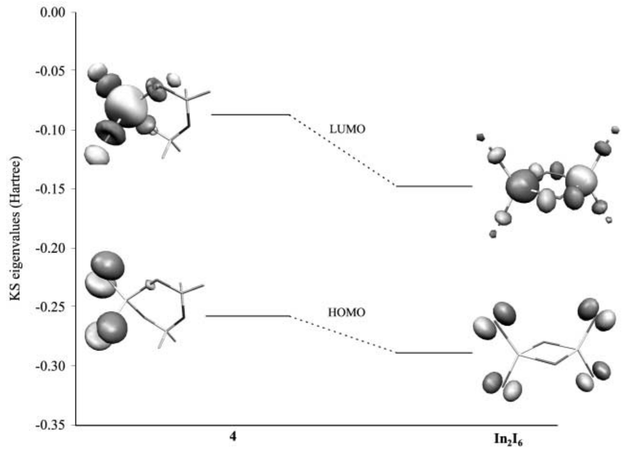

Fig. 5 Comparison of the Kohn–Sham HOMO and LUMO energies calculated for model compound $InL'I_2$ [**L**′ = $(SPH_2)_2N^-$] (**4**) (left) and for In_2I_6 (right).

and In^{II}/In^{I}). Moreover, the antibonding nature of this orbital accounts for the irreversibility of the processes. As far as oxidation is concerned, the composition of the HOMOs in terms of atomic orbitals indicates that the process regards the iodide ions of both species ($2I^-/I_2$). The HOMOs' eigenvalues (ε_{HOMO} = −0.290 and −0.259 Hartree for In_2I_6 and **4**, respectively) account for the different oxidation potentials of **1** and In_2I_6.

Conclusions

To sum up we have shown that the reaction between the adduct **HL**·I_2 and In in Et_2O clearly affords the oxidation of indium to the +3 oxidation state and its complexation to produce In**L**I_2. We have found that this complex readily reacts with HI to yield the anion InI_4^- with the release of **HL**. These two reactions performed in sequence may open new perspectives for the recovery of In^0 from indium-containing materials according to Scheme 1.

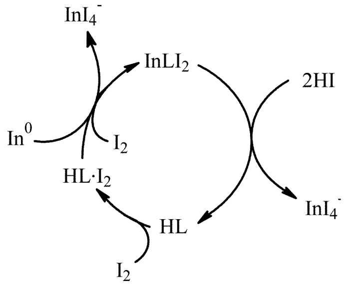

Scheme 1

Experimental

Materials and instrumentation

Reagents were used as purchased from Aldrich. Diethyl ether was distilled over $LiAlH_4$ shortly before use. All reactions were carried out under a dry nitrogen atmosphere.

$^{31}P\{^1H\}$ and ^{115}In NMR (indium-115, spin number I = 9/2, isotopic abundance of 95.72%) spectra were recorded on a Varian Unity 400 MHz spectrometer; chemical shift values were referenced to an external standard of 85% H_3PO_4 (δ_{31P} 0.0), inserted as a sealed co-axial tube, and to an 0.5 mol dm^{-3} solution of $InCl_4^-$ in dichloromethane (δ_{115In} 0.0),[24] respectively. All solution NMR experiments were carried out with NMR tubes with a PTFE valve (Aldrich). ^{31}P NMR MAS spectra were calibrated indirectly through the 85% H_3PO_4 peak (δ 0.0). IR spectra were measured as KBr (4000–400 cm^{-1}) and polyethylene pellets (400–50 cm^{-1}) on a Bruker IFS 55 FT-IR spectrometer. FT-Raman spectra were recorded on a Bruker FRS 100 Fourier-transform Raman spectrometer, operating with a diode-pumped Nd:YAG exciting laser emitting at 1064 nm. Cyclic voltammetry experiments were recorded at room temperature, in anhydrous CH_2Cl_2 or CH_3CN at a scan rate of 100 mV s^{-1}, using a conventional three-electrode cell, consisting of a combined working and counter platinum electrode and a standard Ag/AgCl (in 3.5 mol dm^{-3} KCl; 0.2050 V) reference electrode. The solution was about 1 × 10^{-3} mol dm^{-3} in the complex In**L**I_2, with Bu_4NBF_4 (0.1 mol dm^{-3}) as supporting electrolyte. A stream of argon was passed through the solution prior to the scan. Data were recorded on a computer-controlled EG&G (Princeton Applied Research) potentiostat-galvanostat Model 273 EG&G, using Model 270 electrochemical analysis software. Ultraviolet-visible spectra were recorded on a Varian model Cary 5 UV-Vis-NIR spectrophotometer.

Synthesis

Compounds $(SPPh_2)_2NH$ (**HL**) and $Cs(SPPh_2)_2N$ (**CsL**) were prepared according to ref. 25 and 7*c*, respectively.

InL**I_2 (1).** *Method a.* A mixture of **HL** (0.100 g, 0.222 mmol) and I_2 (0.084 g, 0.333 mmol) in diethyl ether (200 mL) was stirred at 25 °C under N_2 until complete dissolution of the reagents. Indium metal powder (100 mesh) (0.0255 g, 0.222 mmol) was added while stirring. This was continued at room temperature for *ca.* 7 days. The filtered solution was allowed to concentrate at room temperature. The very first crop of crystals which separate from the solution were collected, washed with a mixture of CH_2Cl_2 and n-hexane (1 : 5 v/v), and air dried to give 0.042 g, 0.051 mmol of **1**, yield 23%.

Method b. **HL** (0.100 g, 0.222 mmol) in diethyl ether (50 mL) was added to a solution of indium triiodide (0.110 g, 0.222 mmol) in diethyl ether (100 mL). The mixture was allowed to react at 25 °C under N_2 for *ca.* 7 days. The filtered solution was allowed to concentrate at room temperature. The very first crop of crystals which separate from the solution were collected, washed with a mixture of CH_2Cl_2 and n-hexane (1 : 5 v/v), and air dried to give 0.030 g, 0.036 mmol of **1**, yield 16%. mp 230–232 °C. Anal calcd for $C_{24}H_{20}NP_2S_2I_2In$: C, 35.28; H, 2.47; N, 1.71; S, 7.85%. Found: C, 36.1; H, 2.5; N, 1.8; S, 8.0%. ^{31}P NMR (Et_2O): δ 38.1. IR(KBr): ν(PS)/cm^{-1} 566, 523; ν_{asym}(PNP)/cm^{-1} 1240.

X-Ray crystallography

Crystal data for complex 1. $C_{24}H_{20}I_2InNP_2S_2$, M = 817.11, monoclinic, a = 8.8500(6), b = 17.555(2), c = 18.649(3) Å, β = 93.665(9), U = 2891.4(6) Å^3, T = 298(2) K, space group[26] $P2_1/n$ (No. 14), Z = 4, μ (Mo-Kα) = 3.221 mm^{-1}. 9683 reflections (9147 unique) were collected at room temperature on an Enraf Nonius-CAD4 automatic diffractometer, and 9677 were used in structure refinement (Rint = 0.0109). Intensities were corrected for Lorentz-polarisation effects and empirical absorption (ψ-scan).[27a] The structure was solved by direct methods (SIR-97)[27b] and refined on F_o^2 using the SHELXL-97 program[27c] implemented in the WINGX suite.[27d] All non-hydrogen atoms were refined anisotropically while the hydrogen atoms were treated as idealized contributors and dealt with isotropically. The final value for $R1$ [$wR2$] was 0.0471 [0.1473] on $I > 2\sigma(I)$ [all data] with GoF = 1.087 for 290 parameters and no restraints. The maximum and minimum residual electron density on the final ΔF map are 1.32 and −1.58 e Å^{-3}, respectively. Selected interatomic distances and angles are listed in Table 1.

CCDC reference number 198787.

See http://www.rsc.org/suppdata/dt/b2/b211542e/ for crystallographic data in CIF or other electronic format.

Computations

Density functional calculations (DFT)[23] were carried out on the model complex **4** and on the dimeric form of InI_3 using the suite of programs Gaussian 94,[28] with the hybrid Becke 3LYP functional[29] and Schafer, Horn and Ahlrichs pVDZ basis set[30] for C, H, N, P, and S. For In and I atoms the LANL2DZ basis set was used with effective core potentials (ECP)[31] accounting for 46 inner electron shells. In the case of **4**, SCF convergence was achieved by a quadratic convergence procedure (QC option) based on the Bacskay method.[32] Starting from crystallographic geometrical parameters, geometry optimisations were performed and the results were examined with the Molden 3.6 program.[33] Both quantum mechanically optimised structures were verified by normal-mode harmonic frequency analysis. The NBO charge distribution[34] was calculated for all the examined compounds.

Acknowledgements

This research was financially supported by the "Regione Autonoma della Sardegna". We are grateful to the "Centro Interdipartimentale Grandi Strumenti (C.I.G.S.)" of the University of Modena and Reggio Emilia for providing X-rays analysis equipment.

References and notes

1 (*a*) S. M. Godfrey, C. A. McAuliffe, R. G. Pritchard and J. M. Sheffield, *Inorg. Chim. Acta*, 1999, **292**(2), 213; (*b*) S. M. Godfrey, N. Ho, C. A. McAuliffe and R. G. Pritchard, *Angew. Chem., Int. Ed. Engl.*, 1996, **33**, 2344; (*c*) C. A. McAuliffe, S. M. Godfrey, A. G. Mackie and R. G. Pritchard, *Angew. Chem., Int. Ed. Engl.*, 1992, **31**, 919 and references therein.

2 F. Bigoli, P. Deplano, M. L Mercuri, M. A. Pellinghelli, G. Pintus, A. Serpe and E. F. Trogu, *J. Am. Chem. Soc.*, 2001, **123**, 1788.

3 F. Bigoli, P. Deplano, M. L Mercuri, M. A. Pellinghelli, G. Pintus, M. A. Serpe and E. F. Trogu, *Chem. Commun.*, 1998, 2351.

4 F. Bigoli, P. Deplano, F. A. Devillanova, V. Lippolis, M. L. Mercuri, M. A. Pellinghelli and E. F. Trogu, *Inorg. Chim. Acta*, 1998, **267**, 115.

5 (*a*) C. Silvestru and J. E. Drake, *Coord. Chem. Rev.*, 2001, **223**, 117; (*b*) M. Necas, M. R. S. Foreman, J. Marek, J. D. Woollins and J. Novosad, *New J. Chem.*, 2001, **25**, 1256; (*c*) D. J. Birdsall, A. M. Z. Slawin and J. D. Woollins, *Polyhedron*, 2001, **20**, 125; (*d*) D. J. Birdsall, J. Novosad, A. M. Z. Slawin and J. D. Woollins, *J. Chem. Soc., Dalton Trans.*, 2000, 435; (*e*) D. J. Birdsall, A. M. Z. Slawin and J. D. Woollins, *Inorg. Chem.*, 1999, **38**, 4152; (*f*) D. Cupertino, R. Keyte, A. M. Z. Slawin, D. J. William and J. D. Woollins, *Polyhedron*, 1996, **24**, 4441 and references therein.

6 (*a*) M. J. Baker, M. F. Gilles, A. G. Orpen, M. J. Taylor and R. J. Watt, *J. Chem. Soc., Chem. Commun.*, 1995, 197; (*b*) J. R. Dilworth, J. R. Miller, N. Wheatley, M. J. Baker and J. G. Sunley, *J. Chem. Soc., Chem. Commun.*, 1995, 1579.

7 (*a*) G. L. Abbati, M. C. Aragoni, M. Arca, A. C. Fabretti, F. A. Devillanova, A. Garau, F. Isaia, V. Lippolis and G. Verani, *J. Chem. Soc., Dalton Trans.*, 2001, 1105; (*b*) M. C. Aragoni, M. Arca, A. Garau, F. Isaia, V. Lippolis, G. L. Abbati and A. C. Fabretti, *Z. Anorg. Allg. Chem.*, 2000, **626**, 1454; (*c*) A. M. Z. Slawin, J. Ward, D. J. Williams and J. D. Woollins, *J. Chem. Soc., Chem. Commun.*, 1994, 421; (*d*) R. Rösler, C. Silvestru, G. Espinosa-Pérez, I. Haiduc and R. Cea-Olivares, *Inorg. Chim. Acta*, 1996, **241**, 47; (*e*) O. Siiman and H. B. Gray, *Inorg. Chem.*, 1974, **13**, 1185 and references therein.

8 (*a*) M. Arca, A. Garau, F. A. Devillanova, F. Isaia, V. Lippolis, G. Verani, G. L. Abbati and A. Cornia, *Z. Anorg. Allg. Chem.*, 1999, **625**, 517; (*b*) O. Siiman, C. P. Huber and M. L. Post, *Inorg. Chim. Acta*, 1977, **25**, L 11; (*c*) O. Siiman and J. Vetuskey, *Inorg. Chem.*, 1980, **19**, 1672.

9 (*a*) C. G. Pernin and J. A. Ibers, *Inorg. Chem.*, 2000, **39**, 1216; (*b*) C. G. Pernin and J. A. Ibers, *Inorg. Chem.*, 2000, **39**, 1222.

10 B. C. Ranu, *Eur. J. Org. Chem.*, 2000, **13**, 2347.

11 The three major applications for indium – display devices, low melting-point alloys and solders, and semiconductors – are expected to grow steadily in future years to reach 250 tonnes per year by 2005. Flue dusts and treatable residues from which indium can be recovered is therefore expected to increase too. Source: Roskill, Reports on Metals and Minerals, The economics of Indium, 7th edition, published November 1999. ISBN 0862148359. http://roskill.co.uk/indium.html (Accessed November 2002).

12 M. A. Brown and D. G. Tuck, *Inorg. Chim. Acta*, 1996, **247**, 135.

13 (*a*) R. Cea-Olivares, R. A. Toscano, G. Carreón and J. Valdès-Martinez, *Monatsh. Chem.*, 1992, **123**, 391; (*b*) V. García-Montalvo, R. Cea-Olivares, D. J. Williams and G. Espinoza-Pérez, *Inorg. Chem.*, 1996, **35**, 3948; (*c*) V. García-Montalvo, R. Cea-Olivares, J. Novosad, D. J. Williams, R. A. Toscano and G. Espinoza-Pérez, *Chem. Ber.*, 1996, **129**, 919.

14 (*a*) K. Darwin, L. M. Gilby, P. R. Hodge and B. Piggott, *Polyhedron*, 1999, **18**, 3729; (*b*) R. Cea-Olivares, R. A. Toscano, S. Hernández-Ortega, J. Novosad and V. García-Montalvo, *Eur. J. Inorg. Chem.*, 1999, 1613.

15 S. Husebye and K. Maartmann-Moe, *Acta Chem. Scand., Ser. A*, 1983, **37**, 439.

16 Because of the large quadrupole moment of the indium-115 nucleus, the ^{115}In NMR resonance will be observable only when the nucleus is in a symmetrical environment, and even then typical linewidths are 250–1000 Hz. T. H. Cannon and R. E. Richards, *Trans. Faraday Soc.*, 1966, **62**, 1378.

17 G. P. McQuillan and I. A. Oxton, *Inorg. Chim. Acta*, 1978, **29**, 69.

18 K. F. Purcell and J. C. Kotz, *Inorganic Chemistry*, W. B. Saunders Company, Philadelphia, 1977, ch. 5, pp. 209–212.

19 M. A. Malyarick and S. P. Petrosyants, *Inorg. Chem.*, 1993, **32**, 2265.

20 M. A. Brown, D. G. Tuck and E. J. Wells, *Can. J. Chem.*, 1996, **74**, 1535.

21 InI_3, which has the iodine bridged structure $X_2InX_2InX_2$ in the solid state, and the anion InI_4^- show similar chemical shifts in Et_2O. However, the linewidth in InI_4^- is significantly sharper. The formal negative charge seems to have little effect on the resonance frequency, as both InI_4^- and In_2I_6 involve In(III) tetrahedrally bonded to iodine.[24] Similar results were found for the system InI_3 + I^- in CH_3CN solution: InI_3 0.1 mol dm^{-3}, δ −999, $\Delta\nu_{1/2}$ = 430 Hz; InI_4^- δ −1009, $\Delta\nu_{1/2}$ = 240 Hz[19].

22 A. J. Carthy and D. G. Tuck, *Prog. Inorg. Chem.*, 1975, **19**, 243.

23 T. Ziegler, *Can. J. Chem.*, 1995, **73**, 743.

24 B. R. McGarvey, C. Owens Trudell, D. G. Tuck and L. Victoriano, *Inorg. Chem.*, 1980, **19**, 3432.

25 A. Schmidpeter, R. H. Bohm and H. Groenger, *Angew. Chem.*, 1964, **76**, 870.

26 *International Tables for X-ray Crystallography*, ed. T. Hanh, D. Riedel, Dordrecht, The Netherlands, 1983.

27 (*a*) A. C. T. North, D. C. Phillips and F. S. Mathews, *Acta Crystallogr., Sect. A*, 1968, **24**, 351; (*b*) A. Altomare, M. C. Burla, M. Camall, G. L. Cascarano, C. Giacovazzo, A. Guagliardi, A. G. G. Moliterni, G. Polidori and R. Spagna R, *J. Appl. Crystallogr.*, 1999, **32**, 115; (*c*) G. M. Sheldrick, SHELXL-97, Program for Crystal Structure Refinement (release 97-2), University of Göttingen, Germany, 1997; (*d*) L. J. Farrugia, *J. Appl. Crystallogr.*, 1999, **32**, 837; (*e*) L. J. Farrugia, *J. Appl. Crystallogr.*, 1997, **30**, 565.

28 M. J. Frisch, G. W. Trucks, H. B. Schlegel, P. M. W. Gill, B. G. Johnson, M. A. Robb, J. R. Cheeseman, T. A. Keith, G. A. Petersson, J. A. Montgomery, K. Raghavachari, M. A. Al-Laham, V. G. Zakrzewski, J. V. Ortiz, J. B. Foresman, C. Y. Peng, P. Y. Ayala, M. W. Wong, J. L. Andres, E. S. Replogle, R. Gomperts, R. L. Martin, D. J. Fox, J. S. Binkley, D. J. Defrees, J. Baker, J. P. Stewart, M. Head-Gordon, C. Gonzalez and J. A. Pople, Gaussian 94 (*Revision D.1 & E.1*), Gaussian, Inc., Pittsburgh, PA, 1995.

29 A. D. Becke, *J. Chem. Phys.*, 1993, **98**, 1372.

30 A. Schafer, H. Horn and R. Ahlrichs, *J. Chem. Phys.*, 1992, **97**, 2571.

31 P. J. Hay and W. R. Wadt, *J. Chem. Phys.*, 1985, **82**, 270.

32 G. B. Bacskay, *Chem. Phys.*, 1981, **61**, 385.

33 MOLDEN 3.6, a pre- and post-processing program for molecular and electronic structures, G. Schaftenaar and J. H. Noordik, *J. Comput.-Aided Mol. Des.*, 2000, **14**, 123.

34 A. E. Reed and F. Weinhold, *J. Chem. Phys.*, 1983, **78**, 4066.